HETEROCYCLES, Vol. 99, No. 1, 2019, pp. 238 - 247. © 2019 The Japan Institute of Heterocyclic Chemistry
Received, 29th June, 2018, Accepted, 13th July, 2018, Published online, 20th July, 2018
DOI: 10.3987/COM-18-S(F)16

STRUCTURE–ACTIVITY RELATIONSHIP STUDY OF GATASTATIN BASED ON THE TOPLISS TREE APPROACH

Ichiro Hayakawa,[1]* Shuya Shioda,[2] Takumi Chinen,[3†] Takeo Usui,[3] and Hideo Kigoshi[2]*

[1] Division of Applied Chemistry, Graduate School of Natural Science and Technology, Okayama University, 3-1-1 Tsushima-naka, Kita-ku, Okayama 700-8530, Japan. [2] Department of Chemistry, Graduate School of Pure and Applied Sciences, University of Tsukuba, 1-1-1 Tennodai, Tsukuba 305-8571, Japan. [3] Graduate School of Life and Environmental Sciences, University of Tsukuba, 1-1-1 Tennodai, Tsukuba 305-8571, Japan.
* E-mail: ichiro.hayakawa@okayama-u.ac.jp, kigoshi@chem.tsukuba.ac.jp

[†] Present address: Department of Physiological Chemistry, Graduate School of Pharmaceutical Sciences, University of Tokyo, Tokyo 113-0033, Japan.

This paper is dedicated to Professor Tohru Fukuyama on the occasion of his 70th birthday.

Abstract – Various analogues of gatastatin, a γ-tubulin-specific inhibitor, were designed and synthesized by systematically optimizing the aromatic ring at the O^7-benzyl group in accordance with an operational Topliss tree, and their biological activities were evaluated. Some derivatives showed stronger cytotoxicity against HeLa cells than gatastatin. Especially, the cytotoxicity of the *meta*-chloro derivative was about 18-fold stronger than that of gatastatin. However, these derivatives did not exhibit binding ability to the yeast γ-tubulin small complex or inhibitory activity against α,β-tubulin polymerization. These results suggested that γ-tubulin strongly recognized the unsubstituted phenyl ring of the O^7-benzyl group in gatastatin.

INTRODUCTION

Microtubules are polymers of α,β-tubulin heterodimers. Inhibitors of α,β-tubulin polymerization or depolymerization are cytotoxic against tumor cells. Especially, vinblastine and vincristine, naturally

occurring inhibitors of α,β-tubulin polymerization, are used in cancer therapy.[1] On the other hand, γ-tubulin is a member of the tubulin superfamily and forms the γ-tubulin ring complex (γ-TuRC), which is the starting point of α,β-tubulin polymerization in cells.[2] In light of this phenomenon, γ-tubulin is an attractive target protein for the development of novel types of anticancer drugs.

Glaziovianin A (**1**) is a naturally occurring isoflavone derivative.[3] Previously, we synthesized glaziovianin A (**1**)[4] and revealed from competition-binding experiments that glaziovianin A (**1**) binds to the colchicine site of β-tubulin and inhibits microtubule dynamics in cells.[5] Furthermore, we investigated the structure–activity relationships of glaziovianin A (**1**)[6] and revealed that O^6-benzyl glaziovianin A (**2**) inhibits the α,β-tubulin polymerization more strongly than do known α,β-tubulin inhibitors, such as colchicine and glaziovianin A (**1**).[7,8] O^6-Benzyl glaziovianin A (**2**) also inhibits GTP binding on γ-tubulin. In contrast, O^7-benzyl glaziovianin A (**3**), called gatastatin, does not affect α,β-tubulin polymerization and specifically inhibits γ-tubulin functions including GTP binding, microtubule capping, and microtubule nucleation.[9] To the best of our knowledge, gatastatin (**3**) is the first γ-tubulin-specific inhibitor. It is interesting that glaziovianin A derivatives change their mode of action through benzylation at the O^6 (α,β-tubulin and γ-tubulin inhibitor) or O^7 (γ-tubulin-specific inhibitor) position. Because gatastatin (**3**) specifically inhibits γ-tubulin, we focused on the O^7-benzyl group in gatastatin (**3**) in our structure–activity relationship study. Thus, we planned to synthesize substituted benzyl analogues at the O^7 position in gatastatin (**3**) from our synthetic intermediate **10** (O^7-demethyl glaziovianin A) and to evaluate their biological activities. In this paper, we describe the structure–activity relationship of the O^7-benzyl group in gatastatin (**3**) based on the Topliss tree approach.[10]

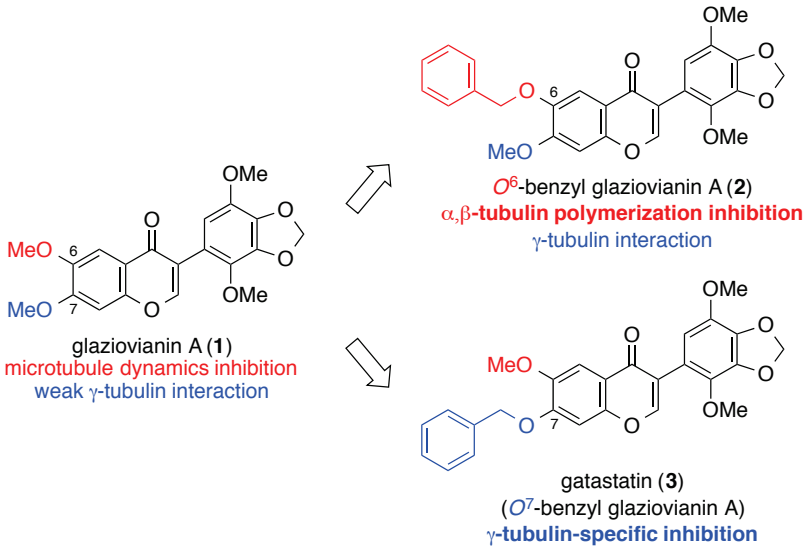

Figure 1. Structures and derivatives of glaziovianin A (**1**)

RESULTS AND DISCUSSION

In our previous work, we established a practical route to synthesize O^7-modified glaziovianin A and used that route to synthesize gatastatin (**3**) (Scheme 1).[4b,9] Thus, we synthesized iodochromone **7** on a gram scale by using the Fries rearrangement as a key step. The Suzuki–Miyaura coupling[11] between iodochromone **7** and pinacol boronate **8**[4b] gave coupling compound **9**, and removal of the THP group of **9** furnished O^7-demethyl glaziovianin A (**10**), which was a common intermediate of O^7-modified glaziovianin A.

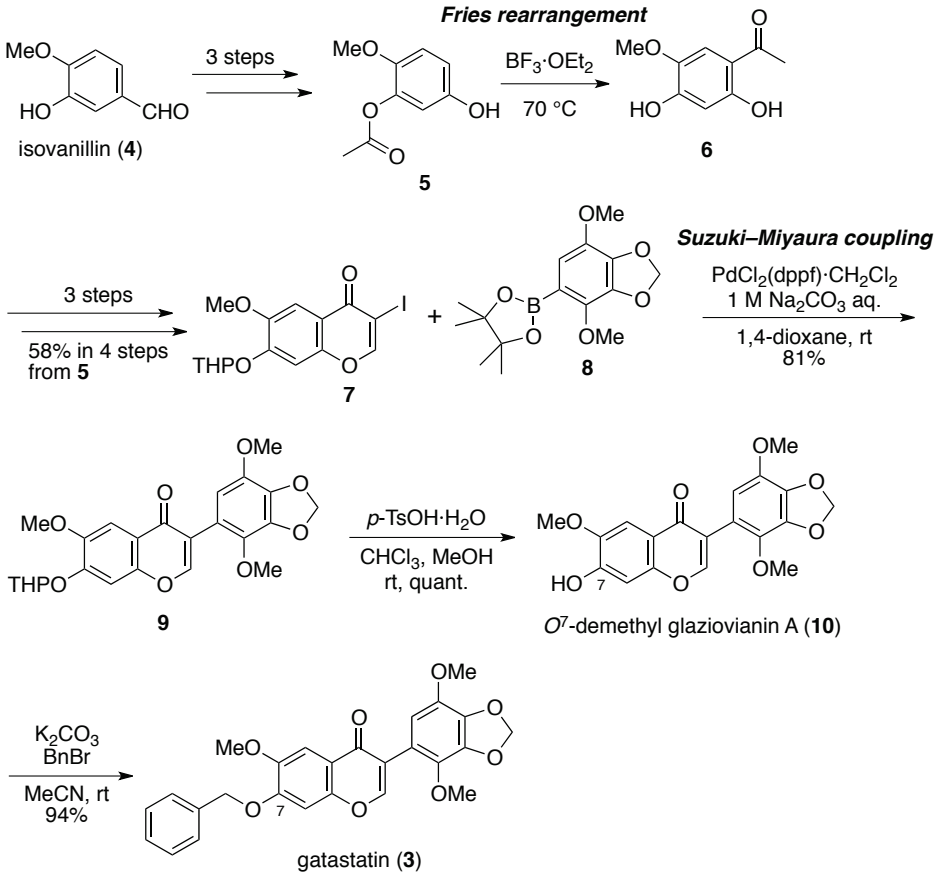

Scheme 1. Previous work: Synthesis of gatastatin (**3**)

We prepared various Topliss derivatives **11**–**17** from our synthetic intermediate **10** via benzylation with various substituted benzyl halides in good yield (95% – quantitative yield, Table 1). In addition, we prepared O^7-benzophenoylmethyl gatastatin (**18**) referring to KPU-406 (pinabulin[12] derivative, Figure 2), which binds to γ-tubulin and inhibits α,β-tubulin polymerization.[9]

Table 1. Synthesis and cytotoxicity against HeLa cells of gatastatin derivatives **11**–**18**

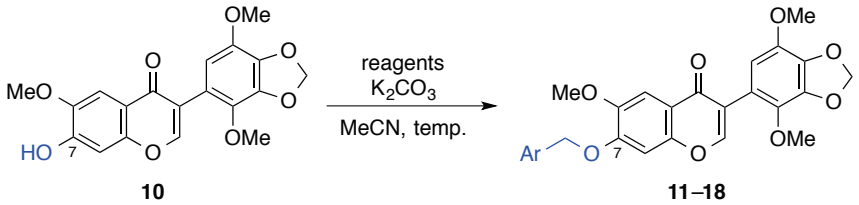

reagent	temp.	product	yield	IC_{50} (μM)[a]
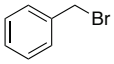	rt	gatastatin (**3**)	94%[b]	12.81 ± 6.26[b]
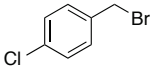	rt	**11**	quant	3.9 ± 1.2
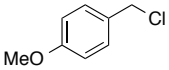	reflux	**12**	95%	3.9 ± 0.2
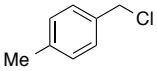	reflux	**13**	quant	10.3 ± 5.2
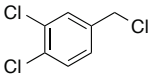	reflux	**14**	quant	2.9 ± 0.7
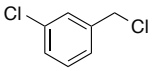	reflux	**15**	quant	0.7 ± 0.3
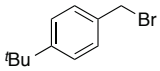	rt	**16**	quant	1.3 ± 0.4
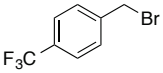	rt	**17**	quant	30 >
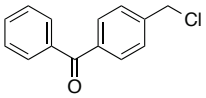	rt	**18**	quant	30 >

[a] Values are expressed as mean ± s.d. from three independent experiments.

[b] Ref. 8

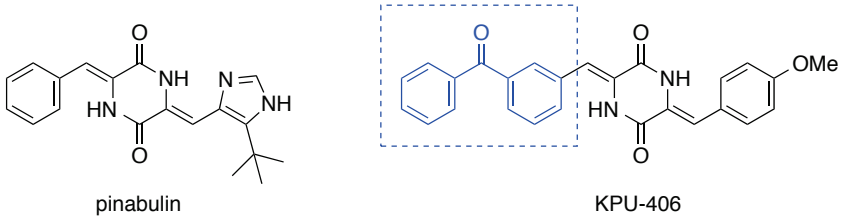

Figure 2. Structures of pinabulin and KPU-406

Because the inhibitory activity of γ-tubulin is generally linked to cytotoxicity, we evaluated the cell growth inhibitory effects of gatastatin derivatives **11**–**18** against HeLa cells as a first screening (Table 1 and Figure 3). According to the Topliss tree approach, the compound with the *para*-chloro substituent on the aromatic ring at the O^7-benzyl group (**11**) was tested for cytotoxicity. *para*-Chloro derivative **11** was more active (IC_{50} = 3.9 μM) than gatastatin (**3**, IC_{50} = 12.8 μM). Following the Topliss tree approach, both branches "M" (more active) and "E" (equiactive) were explored. 3,4-Dichloro derivative **14** indicated almost the same result (IC_{50} = 2.9 μM) compared to *para*-chloro derivative **11**. Next, following branch "E", the activity of *para*-CF_3 derivative **17** was evaluated and found to be noncytotoxic even at 30 μM. In contrast, following branch "E" from the *para*-chloro derivative **11**, we examined the cytotoxicity of *para*-methyl derivative **13**, which showed decreased cytotoxicity (IC_{50} = 10.3 μM). Therefore, we tested *meta*-chloro derivative **15** following branch "L" (less active); **15** showed the strongest cytotoxicity of any derivative in this study (IC_{50} = 0.7 μM).

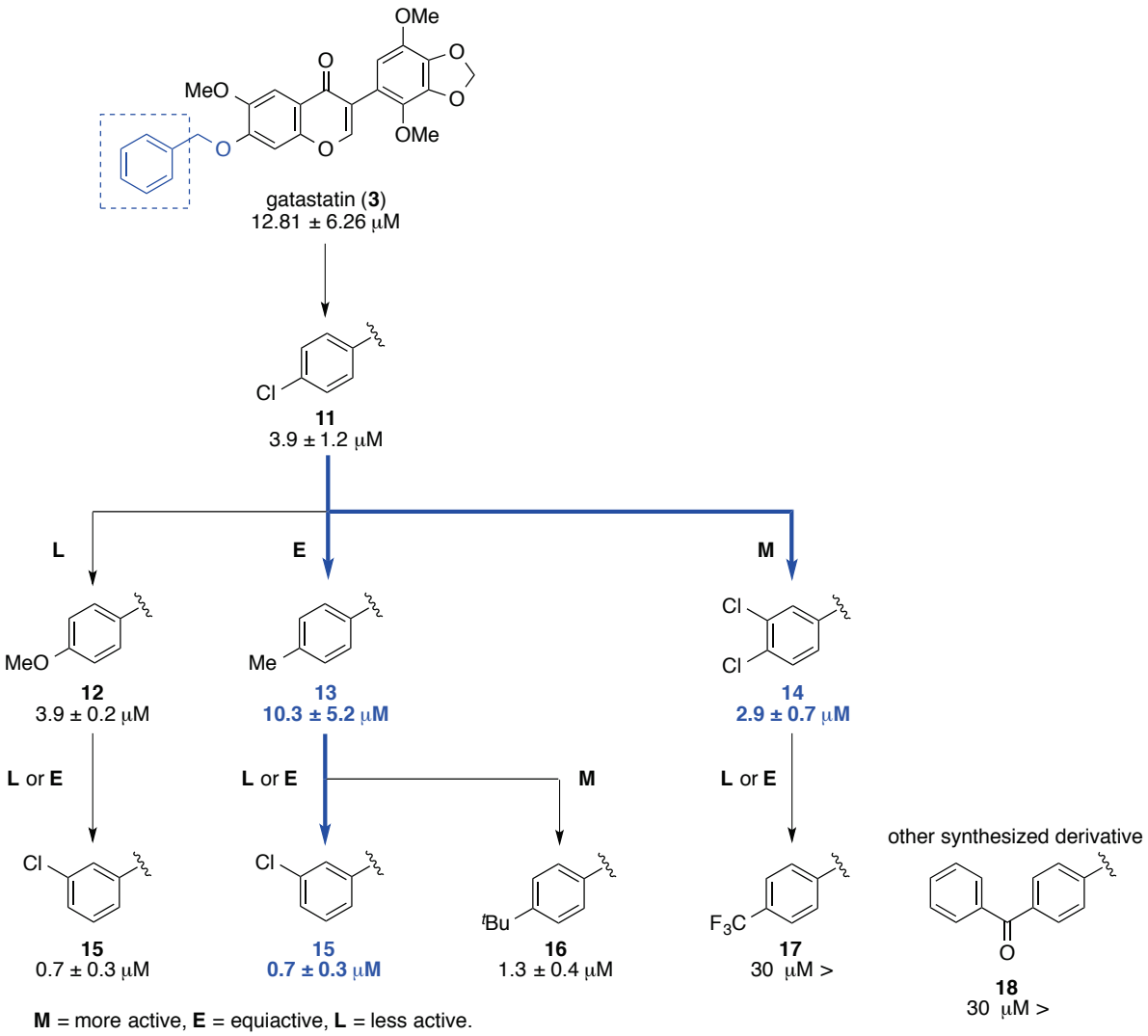

Figure 3. Topliss operational scheme of the substituted benzyl group at the O^7 position in gatastatin (**3**)

The cytotoxicities of derivatives **12** and **16** were stronger than that of gatastatin (**3**). In this manner, we improved the cytotoxicity of gatastatin (**3**) by systematically optimizing the substituents on the aromatic ring at the O^7-benzyl group in gatastatin (**3**) using an operational Topliss tree, thus developing the most cytotoxic derivative **15**. On the other hand, O^7-benzophenoylmethyl gatastatin (**18**) indicated no cytotoxicity even at 30 μM.

We next evaluated the binding ability to the yeast (*S. cerevisiae*) γ-TuSC (γ-tubulin small complex) and the inhibitory activity of α,β-tubulin polymerization of derivatives **11**–**18**. However, none of these derivatives exhibited binding affinity for γ-TuSC in a differential scanning fluorimetry assay (data not shown).[13] In addition, these derivatives showed no inhibitory activity against α,β-tubulin polymerization even at 30 μM, unlike the case with O^6-benzyl glaziovianin A (**2**) (IC_{50} = 2.1 μM).[8] We supposed that these derivatives, such as **11**–**16**, showed cytotoxicity against HeLa cells by interacting not with tubulin but with one or more other target biomolecules. These results suggested that γ-tubulin strictly recognized the unsubstituted phenyl ring of the O^7-benzyl group in gatastatin (**3**) (Figure 4).

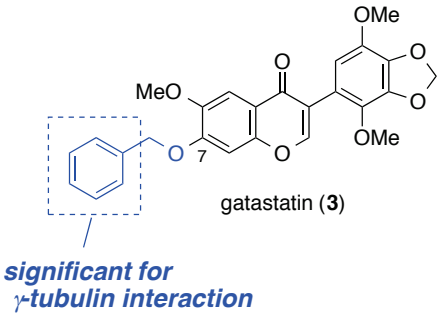

Figure 4. Summary of the structure–activity relationships of gatastatin (**3**)

In conclusion, we have designed gatastatin derivatives by systematically optimizing the substituents on the aromatic ring at the O^7-benzyl group in gatastatin using an operational Topliss tree. Some of these derivatives are more cytotoxic against HeLa cells than gatastatin (**3**). Especially, the cytotoxicity of *meta*-chloro derivative **15** was about 18-fold stronger than that of gatastatin (**3**). However, these derivatives did not exhibit binding ability to the γ-tubulin small complex or inhibitory activity against α,β-tubulin polymerization. On the basis of these results, we presumed that γ-tubulin strictly recognized the unsubstituted phenyl ring of the O^7-benzyl group in gatastatin (**3**). Further studies on the design and synthesis of gatastatin derivatives retaining the O^7-benzyl group for the development of a more effective γ-tubulin-specific inhibitor are under way by our group.

EXPERIMENTAL

Chemistry

General method: All chemicals were used as obtained from commercial supplies unless otherwise noted. Anhydrous MeCN was purchased from Wako Pure Chemical Industries Ltd, and used without further drying. TLC analyses were conducted on E. Merck precoated silica gel 60 F_{254} (0.25 mm layer thickness). Fuji Silysia silica gel BW-820MH was used for column chromatography. Infrared (IR) spectra were recorded on a JASCO FT/IR-230 instrument and only selected peaks are reported in wavenumbers (cm^{-1}). ^1H and ^{13}C NMR spectra were recorded on a Bruker AVANCE 400 spectrometer or a Bruker DPX 400 spectrometer. The ^1H and ^{13}C chemical shifts were referenced to the solvent peaks, δ_H 7.26 (residual $CHCl_3$) and δ_C 77.0 ppm ($CDCl_3$). *J* values are given in Hz. The following abbreviations are used for spin multiplicity: s = singlet, d = doublet, t = triplet, q = quartet, m = multiplet, and br = broad. High resolution ESI (electrospray ionization)/TOF (time-of-flight) mass spectra were recorded on a JEOL AccuTOFCS JMST100CS spectrometer.

Typical procedure for the benzylation of *O*^{7}-demethyl glaziovianin A (10).

7-((4-Chlorobenzyl)oxy)-3-(4,7-dimethoxybenzo[*d*][1,3]dioxol-5-yl)-6-methoxy-4*H*-chromen-4-one (11). To a stirred solution of the *O*^{7}-demethyl glaziovianin A (**10**) (10.0 mg, 26.8 μmol) in MeCN (2.0 mL) were added K_2CO_3 (11.4 mg, 82.4 μmol) and 4-chlorobenzyl bromide (16.3 mg, 79.5 μmol) at room temperature. After being stirred at room temperature for 18 h, the reaction mixture was diluted with saturated aqueous $NaHCO_3$ (2.0 mL) and extracted with $CHCl_3$ (10 mL × 3). The combined extracts were washed with brine, dried (Na_2SO_4), filtered, and concentrated. The crude product was purified by column chromatography on silica gel (700 mg, ^{n}hexane–EtOAc = 3 : 1 → $CHCl_3$) to give *O*^{7}-4-chlorobenzyl gatastatin (**11**) (13.3 mg, quant); IR ($CHCl_3$) 3022, 3018, 1635, 1608, 1502, 1228, 1095 cm^{-1}; ^1H NMR (400 MHz, $CDCl_3$) δ 7.88 (s, 1H), 7.64 (s, 1H), 7.41 (d, *J* = 8.7 Hz, 2H), 7.40 (d, *J* = 8.7 Hz, 2H), 6.87 (s, 1H), 6.51 (s, 1H), 6.02 (s, 2H), 5.22 (s, 2H), 3.99 (s, 3H), 3.87 (s, 3H), 3.84 (s, 3H); ^{13}C NMR (100 MHz, $CDCl_3$) δ 175.4, 153.5, 153.0, 152.0, 148.0, 139.1, 139.0, 137.1, 136.8, 134.2, 134.1, 129.0 (2C), 128.6 (2C), 121.7, 118.2, 118.0, 110.1, 105.3, 101.8, 101.4, 70.4, 60.2, 56.9, 56.4; HRMS (ESI) *m/z* 519.0809, calcd for $C_{26}H_{21}{}^{35}ClNaO_8$ $[M+Na]^+$ 519.0817.

3-(4,7-Dimethoxybenzo[*d*][1,3]dioxol-5-yl)-6-methoxy-7-((4-methoxybenzyl)oxy)-4*H*-chromen-4-one (12). After the column chromatography, the resultant mixture was purified by recycle HPLC [JAIGEL-1H-40 (ϕ20 × 600 mm) and JAIGEL-2H-40 (ϕ20 × 600 mm); flow rate 3.8 mL/min; detection, UV 254 nm; solvent $CHCl_3$] to give *O*^{7}-4-methoxybenzyl gatastatin (**12**) (13.4 mg, 95%). IR ($CHCl_3$) 3021, 3019, 1640, 1608, 1502, 1326, 1228 cm^{-1}; ^1H NMR (400 MHz, $CDCl_3$) δ 7.87 (s, 1H), 7.87 (s, 1H), 7.40 (d, *J* = 8.6 Hz, 2H), 6.93 (d, *J* = 8.6 Hz, 2H), 6.91 (s, 1H), 6.51 (s, 1H), 6.02 (s, 2H), 5.19 (s, 2H), 3.97 (s, 3H), 3.86 (s, 3H), 3.84 (s, 3H), 3.82 (s, 3H); ^{13}C NMR (100 MHz, $CDCl_3$) δ 175.4, 159.8, 153.4

(2C), 152.1, 148.1, 139.2, 139.0, 137.1, 136.8, 129.1 (2C), 127.6, 127.6, 118.1, 118.0, 114.2 (2C), 110.1, 105.1, 101.8, 101.4, 71.0, 60.2, 56.9, 56.4, 55.3; HRMS (ESI) *m/z* 515.1320, calcd for $C_{27}H_{24}NaO_9$ $[M+Na]^+$ 515.1313.

3-(4,7-Dimethoxybenzo[*d*][1,3]dioxol-5-yl)-6-methoxy-7-((4-methylbenzyl)oxy)-4*H*-chromen-4-one (13). IR ($CHCl_3$) 3022, 3016, 1635, 1607, 1501, 1225 cm^{-1}; ^1H NMR (400 MHz, $CDCl_3$) δ 7.87 (s, 1H), 7.62 (s, 1H), 7.35 (d, *J* = 8.0 Hz, 2H), 7.21 (d, *J* = 8.0 Hz, 2H), 6.90 (s, 1H), 6.51 (s, 1H), 6.02 (s, 2H), 5.23 (s, 2H), 3.98 (s, 3H), 3.86 (s, 3H), 3.84 (s, 3H), 2.36 (s, 3H); ^{13}C NMR (100 MHz, $CDCl_3$) δ 175.4, 153.4 (2C), 152.1, 148.1, 139.1, 139.0, 138.2, 137.1, 136.8, 132.6, 129.5 (2C), 127.4 (2C), 121.6, 118.1, 118.0, 110.1, 105.2, 101.8, 101.4, 71.1, 60.2, 56.9, 56.4, 21.2; HRMS (ESI) *m/z* 499.1373, calcd for $C_{27}H_{24}NaO_8$ $[M+Na]^+$ 499.1363.

7-((3,4-Dichlorobenzyl)oxy)-3-(4,7-dimethoxybenzo[*d*][1,3]dioxol-5-yl)-6-methoxy-4*H*-chromen-4-one (14). IR ($CHCl_3$) 3022, 3016, 1635, 1609, 1501, 1225, 1097 cm^{-1}; ^1H NMR (400 MHz, $CDCl_3$) δ 7.88 (s, 1H), 7.64 (s, 1H), 7.58 (d, *J* = 1.9 Hz, 1H), 7.48 (d, *J* = 8.2 Hz, 1H), 7.31 (dd, *J* = 8.2, 1.9 Hz, 1H), 6.86 (s, 1H), 6.51 (s, 1H), 6.02 (s, 2H), 5.19 (s, 2H), 3.99 (s, 3H), 3.87 (s, 3H), 3.85 (s, 3H); ^{13}C NMR (100 MHz, $CDCl_3$) δ 175.4, 153.5, 152.7, 151.9, 148.0, 139.2, 139.0, 137.2, 136.8, 135.9, 133.1, 132.5, 130.8, 129.2, 126.5, 121.8, 118.4, 118.0, 110.1, 105.5, 101.9, 101.5, 71.1, 60.2, 56.9, 56.4; HRMS (ESI) *m/z* 553.0416, calcd for $C_{26}H_{20}{}^{35}Cl_2NaO_8$ $[M+Na]^+$ 553.0427.

7-((3-Chlorobenzyl)oxy)-3-(4,7-dimethoxybenzo[*d*][1,3]dioxol-5-yl)-6-methoxy-4*H*-chromen-4-one (15). IR ($CHCl_3$) 3022, 3016, 1635, 1609, 1502, 1225, 1097 cm^{-1}; ^1H NMR (400 MHz, $CDCl_3$) δ 7.88 (s, 1H), 7.64 (s, 1H), 7.57 (s, 1H), 7.34 (m, 3H), 6.87 (s, 1H), 6.51 (s, 1H), 6.02 (s, 2H), 5.22 (s, 2H), 4.00 (s, 3H), 3.87 (s, 3H), 3.84 (s, 3H); ^{13}C NMR (100 MHz, $CDCl_3$) δ 175.4, 153.5, 153.0, 152.0, 148.0, 139.2, 139.0, 137.7, 137.1, 136.8, 134.8, 130.1, 128.6, 127.3, 125.2, 121.8, 118.3, 118.0, 110.1, 105.4, 101.8, 101.4, 70.3, 60.2, 56.9, 56.4; HRMS (ESI) *m/z* 519.0809, calcd for $C_{26}H_{21}{}^{35}ClNaO_8$ $[M+Na]^+$ 519.0817.

7-((4-(*tert*-Butyl)benzyl)oxy)-3-(4,7-dimethoxybenzo[*d*][1,3]dioxol-5-yl)-6-methoxy-4*H*-chromen-4-one (16). IR ($CHCl_3$) 3022, 3016, 1635, 1607, 1502, 1228 cm^{-1}; ^1H NMR (400 MHz, $CDCl_3$) δ 7.88 (s, 1H), 7.69 (s, 1H), 7.42 (d, *J* = 8.6 Hz, 2H), 7.40 (d, *J* = 8.6 Hz, 2H), 6.92 (s, 1H), 6.52 (s, 1H), 6.02 (s, 2H), 5.22 (s, 2H), 3.98 (s, 3H), 3.86 (s, 3H), 3.84 (s, 3H), 1.33 (s, 9H); ^{13}C NMR (100 MHz, $CDCl_3$) δ 175.4, 153.5, 153.4, 152.1, 151.4, 148.1, 139.2, 139.0, 137.1, 136.8, 132.5, 127.2 (2C), 125.8 (2C), 121.2, 118.1, 118.0, 110.1, 105.2, 101.9, 101.3, 71.1, 60.2, 56.9, 56.4, 34.6, 31.3 (3C); HRMS (ESI) *m/z* 541.1833, calcd for $C_{30}H_{30}NaO_8$ $[M+Na]^+$ 541.1833.

3-(4,7-Dimethoxybenzo[*d*][1,3]dioxol-5-yl)-6-methoxy-7-((4-(trifluoromethyl)benzyl)oxy)-4*H*-chromen-4-one (17). IR ($CHCl_3$) 3021, 3019, 1640, 1608, 1502, 1326, 1228 cm^{-1}; ^1H NMR (400 MHz, $CDCl_3$) δ 7.88 (s, 1H), 7.67 (d, *J* = 8.2 Hz, 2H), 7.65 (s, 1H), 7.59 (d, *J* = 8.2 Hz, 2H), 6.87 (s, 1H), 6.51 (s, 1H), 6.02 (s, 2H), 5.30 (s, 2H), 4.00 (s, 3H), 3.86 (s, 3H), 3.84 (s, 3H); ^{13}C NMR (100 MHz, $CDCl_3$) δ

175.4, 153.5, 152.8, 151.9, 148.0, 139.7, 139.1, 139.0, 137.1, 136.8, 130.6 (q, $^2J_{CF}$ = 32.0 Hz), 127.3 (2C), 125.6 (q, $^3J_{CF}$ = 4.0 Hz, 2C), 124.0 (q, $^1J_{CF}$ = 270.4 Hz), 121.8, 118.4, 118.0, 110.1, 105.5, 101.8, 101.4, 70.2, 60.2, 56.9, 56.4; HRMS (ESI) *m/z* 553.1076, calcd for $C_{27}H_{21}F_3NaO_8$ $[M+Na]^+$ 553.1081.

7-((4-Benzoylbenzyl)oxy)-3-(4,7-dimethoxybenzo[*d*][1,3]dioxol-5-yl)-6-methoxy-4*H*-chromen-4-one (18). IR ($CHCl_3$) 3021, 3009, 1642, 1608, 1502, 1228 cm^{-1}; ^1H NMR (400 MHz, $CDCl_3$) δ 7.88 (s, 1H), 7.85 (d, *J* = 8.1 Hz, 2H), 7.81 (d, *J* = 8.1 Hz, 2H), 7.66 (s, 1H), 7.59 (d, *J* = 7.6 Hz, 2H), 7.59 (t, *J* = 7.3 Hz, 1H), 7.49 (dd, *J* = 7.3, 7.6 Hz, 2H), 6.90 (s, 1H), 6.52 (s, 1H), 6.02 (s, 2H), 5.34 (s, 2H), 4.00 (s, 3H), 3.87 (s, 3H), 3.85 (s, 3H); ^{13}C NMR (100 MHz, $CDCl_3$) δ 196.1, 175.4, 153.5, 153.0, 152.0, 148.1, 140.2, 139.2, 139.0, 137.6, 137.4, 137.2, 136.8, 132.5, 130.6 (2C), 130.0 (2C), 128.3 (2C), 126.8 (2C), 121.7, 118.3, 118.0, 110.1, 105.5, 101.8, 101.5, 70.5, 60.2, 56.9, 56.5; HRMS (ESI) *m/z* 589.1480, calcd for $C_{33}H_{26}NaO_9$ $[M+Na]^+$ 589.1469.

Biology

Calculation of IC_{50} value: HeLa cells were grown in DMEM supplemented with 10% FBS, 100 units/mL penicillin, and 100 μg/mL streptomycin in a humidified atmosphere containing 5% CO_2. Various concentrations of each compound were then added and incubated for 48 h. Cell growth was determined using WST-8 cell counting kit (Dojindo) and IC_{50} value was calculated.

ACKNOWLEDGEMENTS

This work was supported by a Grants-in-Aid for Scientific Research (C) (Grant Number JP17K01949) from the Japan Society for the Promotion of Science (JSPS). I.H. thanks the Okayama Foundation for Science and Technology for financial support.

REFERENCES AND NOTES

1. Review: C. Dumontet and M. A. Jordan, *Nat. Rev. Drug Discov.*, 2010, **9**, 790.
2. Review: T. C. Lin, A. Neuner, and E. Schiebel, *Trends Cell Biol.*, 2015, **25**, 296.
3. A. Yokosuka, M. Haraguchi, T. Usui, S. Kazami, H. Osada, T. Yamori, and Y. Mimaki, *Bioorg. Med. Chem. Lett.*, 2007, **17**, 3091.
4. (a) I. Hayakawa, A. Ikedo, and H. Kigoshi, *Chem. Lett.*, 2007, **36**, 1382; (b) I. Hayakawa, S. Shioda, A. Ikedo, and H. Kigoshi, *Bull. Chem. Soc. Jpn.*, 2014, **87**, 544.
5. T. Chinen, S. Kazami, Y. Nagumo, I. Hayakawa, A. Ikedo, M. Takagi, A. Yokosuka, N. Imamoto, Y. Mimaki, H. Kigoshi, H. Osada, and T. Usui, *ACS Chem. Biol.*, 2013, **8**, 884.
6. I. Hayakawa, A. Ikedo, T. Chinen, T. Usui, and H. Kigoshi, *Bioorg. Med. Chem.*, 2012, **20**, 5745.
7. In this paper, we name *O*-demethyl-*O*-benzyl glaziovianin or gatastatin derivatives as *O*-benzyl

glaziovianins or gatastatins, respectively, for simplification.

8. I. Hayakawa, S. Shioda, T. Chinen, T. Hatanaka, H. Ebisu, A. Sakakakura, T. Usui, and H. Kigoshi, *Bioorg. Med. Chem*., 2016, **24**, 5639.
9. T. Chinen, P. Liu, S. Shioda, J. Pagel, B. Cerikan, T. Lin, O. Gruss, Y. Hayashi, H. Takeno, T. Shima, Y. Okada, I. Hayakawa, Y. Hayashi, H. Kigoshi, T. Usui, and E. Schiebel, *Nat. Commun*., 2015, **6**, 8722.
10. J. G. Topliss, *J. Med. Chem*., 1972, **15**, 1006.
11. Y. Hoshino, N. Miyaura, and A. Suzuki, *Bull. Chem. Soc. Jpn*., 1988, **61**, 3008.
12. Y. Hayashi, H. Takeno, T. Chinen, K. Muguruma, K. Okuyama, A. Taguchi, K. Takayama, F. Yakushiji, M. Miura, T. Usui, and Y. Hayashi, *ACS Med. Chem. Lett*., 2014, **5**, 1094 and references cited therein.
13. F. H. Niesen, H. Berglund, and M. Vedadi, *Nat. Protoc.*, 2007, **2**, 2212.